

MedChemComm

Accepted Manuscript



This is an *Accepted Manuscript*, which has been through the Royal Society of Chemistry peer review process and has been accepted for publication.

Accepted Manuscripts are published online shortly after acceptance, before technical editing, formatting and proof reading. Using this free service, authors can make their results available to the community, in citable form, before we publish the edited article. We will replace this *Accepted Manuscript* with the edited and formatted *Advance Article* as soon as it is available.

You can find more information about *Accepted Manuscripts* in the [Information for Authors](#).

Please note that technical editing may introduce minor changes to the text and/or graphics, which may alter content. The journal's standard [Terms & Conditions](#) and the [Ethical guidelines](#) still apply. In no event shall the Royal Society of Chemistry be held responsible for any errors or omissions in this *Accepted Manuscript* or any consequences arising from the use of any information it contains.

CONCISE ARTICLE

Exploring the Recognition Pathway at the Human A_{2A} Adenosine Receptor of the Endogenous Agonist Adenosine using Supervised Molecular Dynamics Simulations.

Cite this: DOI: 10.1039/x0xx00000x

Received 12th January 2015,
Accepted 00th January 2015

DOI: 10.1039/x0xx00000x

www.rsc.org/

Davide Sabbadin, Antonella Ciancetta, Giuseppe Deganutti, Alberto Cuzzolin, and Stefano Moro*

Adenosine is a naturally occurring purine nucleoside that exerts a variety of important biological functions through the activation of four G protein-coupled receptors (GPCRs) isoforms, namely the A₁, A_{2A}, A_{2B} and A₃ adenosine receptors (ARs). Recently, the X-Ray structure of adenosine-bound hA_{2A} AR has been solved, by providing precious structural details on receptor recognition and activation mechanisms. To date, however, little is still known about the possible recognition pathway the endogenous agonist might go through while approaching the hA_{2A} AR from the extracellular environment. In the present work, we report on adenosine-hA_{2A} AR recognition pathway through the analysis of a series of Supervised Molecular Dynamics (SuMD) trajectories. Interestingly, a possible energetically stable meta-binding site has been detected and characterized.

Introduction

Adenosine is a naturally occurring purine nucleoside that forms primarily from the metabolism of adenosine triphosphate (ATP), both intracellularly and extracellularly.¹ Consequently, the extracellular levels of adenosine are regulated by its synthesis, metabolism, release and uptake.^{1,2} Adenosine exerts pleiotropic functions throughout the body. In the central nervous system (CNS), the nucleoside plays important functions, such as: modulation of neurotransmitter release, synaptic plasticity and neuroprotection in ischemic, hypoxic and oxidative stress events.^{1,3,4} In addition, adenosine plays different roles in a large variety of tissues. In the cardiovascular system, adenosine produces either vasoconstriction or vasodilation of veins and arteries. Moreover, adenosine regulates T cell proliferation and cytokine production, inhibits lipolysis and stimulates bronchoconstriction.^{1,3,4}

Adenosine mediates its biological effects by recognizing four G protein-coupled receptors (GPCRs) isoforms, namely the A₁, A_{2A}, A_{2B} and A₃ adenosine receptors (ARs). Each subtype has a unique pharmacological profile, tissue distribution and effector coupling.^{1,4} Considering receptor sequence similarity, among the human ARs (hARs), the most similar are the A₁ and A₃ ARs (49% similarity), and the A_{2A} and A_{2B} ARs (59% similarity). Conversely, the A₁, A_{2A} and A₃ ARs possess relatively high affinity for adenosine whereas the A_{2B} AR shows relatively lower affinity for adenosine, as summarized in Table 1.

Recently, the crystallographic structure of adenosine-bound hA_{2A} AR has been solved (PDB code: 2YDO).⁵ Although this structural data is extremely precious to interpret both receptor recognition and activation mechanisms of the endogenous agonist, little is still known about the possible recognition pathway between adenosine coming from the extracellular environment and the hA_{2A} AR embedded in the cytoplasmic membrane. In this context, Supervised Molecular Dynamics (SuMD) has been recently presented as an alternative computational method, that allows the exploration of ligand–receptor recognition pathway investigations in a nanosecond (ns) time scale.⁶ In addition to speeding up the acquisition of the ligand–receptor recognition trajectory, this approach facilitates the identification and the structural characterization of multiple binding events (such as meta-binding, allosteric, and orthosteric sites) by taking advantage of the all-atom MD simulations accuracy of a GPCR–ligand complex embedded into explicit lipid–water environment.⁶

In the present study, in order to better understand how adenosine approaches the orthosteric binding site of the hA_{2A} AR, its recognition pathway has been described through the analysis of a series of SuMD trajectories. Interestingly, a possible energetically stable meta-binding site has been detected and characterized. The meta-binding site concept was introduced several year ago to describe those binding events that chronologically anticipate the orthosteric binding event.⁷

Table 1 Adenosine affinities at the four receptor subtypes.

	hA ₁ , Ki (nM)	hA _{2A} , Ki (nM)	hA _{2B} ^a	hA ₃
Adenosine ^b	ca. 100	310	15,000	290

^a data from functional studies.^b ref. 4.

Results and discussion

As anticipated, recently the crystallographic structure of adenosine-bound hA_{2A} AR has been solved. The tentative to apply MD methodologies to address the problem of ligand dissociation from its receptor is subject to some limitations. First of all, ligand dissociation dynamics is usually a slow event in comparison to the timescales accessible to current simulation techniques and computer resources. This does not mean necessarily that the actual event of ligand dissociation takes so long, but it is clear that conformational sampling cannot be done effectively in a conventional MD simulation. On the other hand, the recognition process between a ligand and its receptor is a very rare event to describe at the molecular level and, even with the recent GPU-based computing resources, it is necessary to carry out classical molecular dynamics (MD) experiments in a long microsecond time scale.⁷ For this reason, in order to better understand how adenosine approaches the orthosteric binding site of the hA_{2A} AR, its recognition pathway was explored using a SuMD study (Video 1).

In particular, following the ligand recognition pathway emerged by the analysis of SuMD trajectories (Fig. 1 and Video 1), the third extracellular loop (EL3) of hA_{2A} AR plays an essential role in directing the agonist toward the orthosteric binding site. In particular, His264, Ala265, Pro266 (EL3) and Leu267 (7.32) (Fig.1, panel A) establish favourable hydrophobic contacts with the adenine core of adenosine. Such interactions orient the ribose ring towards the entrance of the orthosteric binding site. The hydroxyl group in C3' position of the ribose ring is engaged in a direct hydrogen bond interaction with Glu169 (EL2). Not surprisingly, the described extracellular site corresponds to the previously reported meta-binding site located in EL3,^{6,7} that enables high-potency hA_{2A} AR antagonists, such as ZM 241385; 6-(2,6-dimethylpyridin-4-yl)-5-phenyl-1,2,4-triazin-3-amine (T4G); and 4-(3-amino-5-phenyl-1,2,4-triazin-6-yl)-2-chlorophenol (T4E), to reach the orthosteric binding cleft from the extracellular vestibule. As already described, once the antagonists reach the orthosteric binding site, they adopt binding conformations that match the geometric positions observed in the corresponding X-ray structures.⁶

By approaching the orthosteric binding site, adenosine explores receptor-bound states that only partially overlap - RMSD < 3.5 Å - (Figure 1, panel B-C) with the crystallographic bound conformation. In such conformational states, the ribose moiety explores the bottom part of the binding pocket ("ribose-down" conformation) and is in close contact with Thr88 (3.36). Glu169 (EL2) and Asn53 (6.55) are involved in key polar interactions with the endo and exo-cyclic nitrogen atoms of the

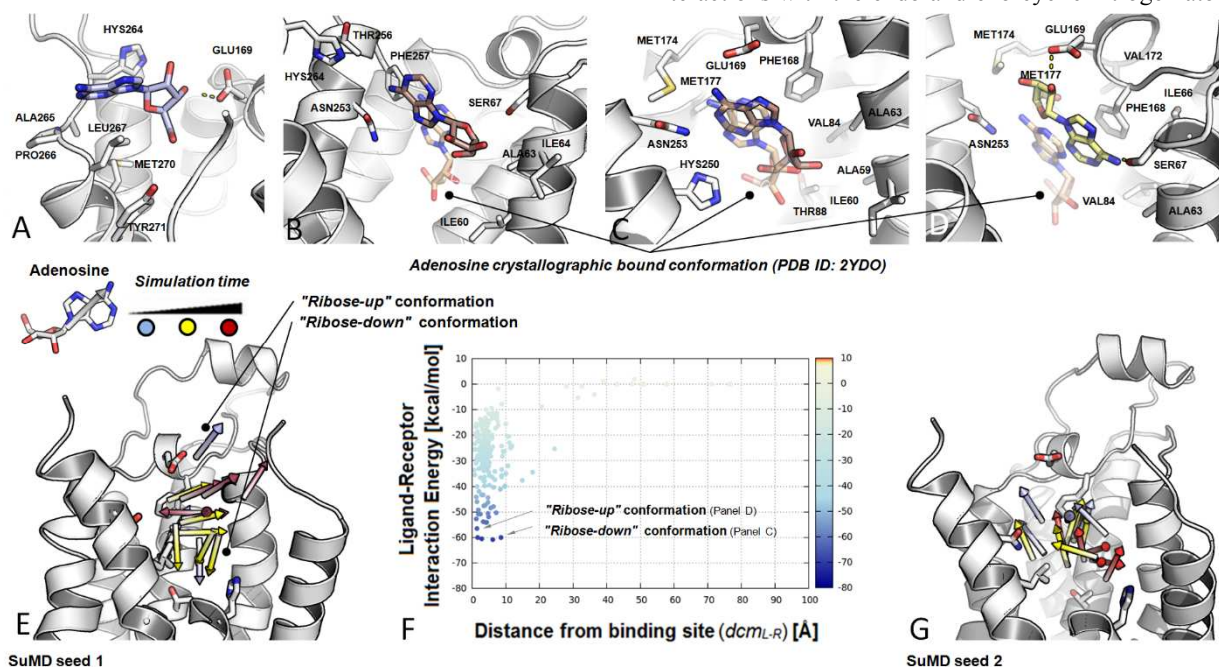


Fig. 1 (Panel A to D) - Overview of multiple adenosine binding conformation inside the hA_{2A} AR binding pocket generated from SuMD simulation trajectories in comparison with X-Ray crystal structure, PDB ID: 2YDO (wheat sticks). Stick colouring scheme is based on simulation progression (time). Hydrogen atoms are not displayed, whereas hydrogen bond interactions are highlighted as yellow dashed lines. (Panel E and G) Overview of multiple discrete binding states that occurs during ligand-receptor recognition. Arrow colouring scheme is based on simulation progression (time). Receptor ribbon representation is viewed from the membrane side facing trans-membrane domain 6 (TM6) and transmembrane domain 7 (TM7). (Panel F) Ligand-receptor interaction energy landscape for the nonbiased adenosine-hA_{2A} AR recognition process. Overview of the most energetically stable binding conformation of adenosine inside the hA_{2A} AR binding pocket are highlighted by arrow. Interaction energy values are expressed in kcal/mol.

aromatic core. Hydrophobic interactions are established with Met174 (5.35), Met177 (5.38), Ala59 (2.57), Ala63 (2.61), Val84 (3.32) and Ile160 (E12). In particular, Phe168 (EL2) is involved in π -stacking interaction with the adenine core.

Notably, the role of several key residues (such as for example Thr88 (3.36), Phe168 (EL2) and Met177 (5.38)) herein highlighted is consistent with the available mutagenesis data for agonist binding, which have been recently analysed and clarified by means of MD/FEP calculations.⁸

As reported in Fig. 1, panel D-F, once inside the orthosteric site, adenosine dynamically flips between two different binding modes: the one above reported - the so-called "ribose-down" conformation - and a "ribose-up" conformation (Figure 1, panel D) where the ribose moiety is directed towards the extracellular space. The hydroxyl group, attached at the C2' position of the ribose ring, establishes a hydrogen-bond interaction with Glu169 (EL2) and the exo-cyclic nitrogen atom of the adenine ring interacts with the Ser67 (2.65) side chain. The agonist aromatic ring is involved in a π -stacking interaction with Phe168 (EL2). Val84 (3.32), Ala63 (2.61) and Met174 (5.35) are responsible of the majority of non-polar ligand-receptor contacts.

Therefore, although the described ligand-receptor contacts provide sufficient energetic protein-ligand complex stabilization to reach global protein-ligand interaction energy minimum (Figure 1, panel F), the recognition of the agonist is not accompanied by subsequent stabilization of the ligand conformation within the orthosteric site, as adenosine dynamically flips between the "ribose down" and "ribose up" binding modes (Figure 1, panel E). Therefore, as also elucidated by a clustering analysis of the space explored by adenosine during the binding pathway, the agonist recognition process does not show the same behaviour of potent hA_{2A} AR antagonists. Adenosine binding profile, instead, is more similar to the one observed for a weak binder such as caffeine (Fig. 1, panel F).⁶ Moreover, this peculiar conformational landscape along with the emerged major interaction sites, which anticipate the orthosteric binding site, are independent from ligand placement and orientation at the beginning of the SuMD simulation (Fig. 1, panel G).

Experimental

General.

The numbering of the amino acids follows the arbitrary scheme by Ballesteros and Weinstein: each amino acid identifier starts with the helix number, followed by the position relative to a reference residue among the most conserved amino acids in that helix, to which the number 50 is arbitrarily assigned.⁹

Trajectory analysis, figure and video generation have been performed using several functionalities implemented by Visual Molecular Dynamics,¹⁰ WORDOM,¹¹ the PyMOL Molecular Graphics System, Version 1.5.0.4 Schrödinger, LLC (<http://www.pymol.org/>) and the GnuPlot graphic utility (<http://www.gnuplot.info/>). Ligand-hA_{2A} AR interaction

energies were calculated extrapolating the non-bonded energy interaction term of CHARMM27 Force Field¹² using NAMD.¹³

Computational facilities.

All computations were performed on a hybrid CPU/GPU cluster. Molecular dynamics simulation have been performed with a 2 NVIDIA GTX 680 and 3 NVIDIA GTX 780 GPU cluster engineered by Acellera.¹⁴

Human A_{2A} Adenosine Receptor-ligand complex preparation.

The selected agonist-bound crystal structures (PDB IDs: 2YDO⁵) and the FASTA sequence of the hA_{2A} AR (Uniprot ID: P29274) were retrieved from the RCSB PDB database¹⁵ (<http://www.rcsb.org>) and the UniProtKB/Swiss-Prot,¹⁶ respectively. Co-crystallized ligand structure was extracted from the orthosteric binding site and randomly placed in the space above the receptor, at least 40 Å away from protein atoms. Ionization states and hydrogen positions were assigned by using MOE-sd wash utility (pH 7.0). The FASTA sequence was aligned, using BLAST (Blosum 62 matrix),¹⁷ with the template sequence. Backbone and conserved residues coordinates were copied from the template structure, whereas newly modelled regions and non-conserved residues side chains were modelled and energetically optimized by using CHARMM 27 force field¹⁸ until a *r.m.s.* of conjugate gradient < 0.05 kcal·mol⁻¹·Å⁻¹ was reached. Missing loop domains were constructed by the loop search method implemented in Molecular Operating Environment (MOE, version 2012.10) program¹⁹ on the basis of the structure of compatible fragments found in the Protein Data Bank. N-terminal and C-terminal were deleted if their lengths exceeded those found in the crystallographic template. The "Protonate-3D" tool²⁰ was used to appropriately assign ionization states and hydrogen positions to the build models. Then, the structures were subjected to energy minimization with CHARMM 27 force field⁴ until the *r.m.s.* of conjugate gradient was < 0.05 kcal·mol⁻¹·Å⁻¹. Protein stereochemistry evaluation was then performed by employing several tools (Ramachandran and χ plots measure j/ψ and χ_1/χ_2 angles, clash contacts reports) implemented in the MOE suite.¹⁹

Receptor membrane embedding and system preparation.

Receptors were embedded in a 1-palmitoyl-2-oleoyl-sn-glycero-3-phosphocholine (POPC) lipid bilayer (85x85 Å wide) and placed into the membrane according to the suggested orientation reported in the "Orientations of Proteins in Membranes (OPM)" database²¹ for the hA_{2A} AR in complex with the antagonist T4G (PDB ID: 2YDV⁷). Overlapping lipids (within 0.6 Å) were removed upon insertion of the protein. The prepared systems were solvated with TIP3P water²² using the program Solvate 1.0²³ and neutralized by Na⁺/Cl⁻ counter-ions to a final concentration of 0.154 M. The total number of atoms per system was approximately 75000. Membrane MD simulations were carried out on a GPU cluster with the ACEMD program using the CHARMM27 Force Field¹⁸ and periodic boundaries conditions. Initial parameters for the

ligands were derived from the CHARMM General Force Field for organic molecules.^{24,25} The system was equilibrated using a stepwise procedure. In the first stage, to reduce steric clashes due to the manual setting up of the membrane-receptor system, a 500 steps conjugate-gradient minimization was performed. Then, to allow lipids to reach equilibrium, water molecules to diffuse into the protein cavity and to avoid ligand-receptor interaction in the equilibration phase, protein and ligand atoms were restrained for the first 8 ns by a force constant of 1 kcal/mol·Å². Then side chains were set free to move, while gradually reducing the force constant to 0.1 kcal/mol·Å² to the ligand and alpha carbon atoms up to 9 ns. Temperature was maintained at 298 K using a Langevin thermostat with a low damping constant of 1 ps⁻¹, and the pressure was maintained at 1 atm using a Berendsen barostat. Bond lengths involving hydrogen atoms were constrained using the M-SHAKE algorithm²⁶ with an integration timestep of 2 fs. Harmonical constraints were then removed and Supervised MD was conducted in a NVT ensemble. Long-range Coulomb interactions were handled using the particle mesh Ewald summation method (PME)²⁷ with grid size rounded to the approximate integer value of cell wall dimensions. A non-bonded cutoff distance of 9 Å with a switching distance of 7.5 Å was used. In order to assess the biophysical validity of the built systems, the average area per lipid headgroup (APL) and bilayer thickness measurements for each built system was measured using Grid-MAT-MD.²⁸ The corresponding calculated averaged area per lipid headgroup of the extracellular and intracellular leaflet during the production phase for all simulations were in agreement with the experimental values measured for 1-palmitoyl-2-oleoyl-sn-glycero-3-phosphocholine (POPC) lipid bilayers.²⁹

Conclusions

In the present work, we have carried out SuMD experiments to elucidate the recognition pathway of the naturally occurring purine nucleoside adenosine by the hA_{2A} AR. The analysis of the SuMD trajectories revealed that residues located in the third extracellular loop play an essential role in orienting the ribose ring of agonist toward the entrance of orthosteric site, thus representing a possible energetically stable meta-binding site.

Our analysis has also revealed that, once reached the orthosteric site, adenosine experiences a dynamically flip between two different binding modes: the "ribose-down" and the "ribose-up" conformation, with the ribose moiety pointing towards the intracellular and extracellular space, respectively.

Consequently, the adenosine binding profile resulting from our analysis resembles the one of a weak binder rather than the one previously observed for potent hA_{2A} AR antagonists.

Further work is undergoing in our lab to better elucidate the role of the meta-binding site that has been detected and characterized in this study. In particular, SuMD simulations with adenosine- hA_{2A} AR 2:1 stoichiometry are currently under evaluation. Moreover, we are carrying out a comprehensive SuMD exploration of the recognition pathway of adenosine

against all other adenosine receptor subtypes to clarify the experimental selectivity profile provided by the natural agonist.

Acknowledgements

This work has been supported with financial support from the University of Padova, Italy, and the Italian Ministry for University and Research, Rome, Italy (MIUR, PRIN2008: protocol number 200834TC4L_002). S.M. is also very grateful to Chemical Computing Group and Acellera for the scientific and technical partnership. S.M. participates in the European COST Action CM1207 (GLISTEN).

Notes and references

^a *Molecular Modeling Section (MMS), Dipartimento di Scienze del Farmaco, Università di Padova, via Marzolo 5, I-35131 Padova, Italy*

Electronic Supplementary Information (ESI) available: Video file of the adenosine-hA_{2A} AR recognition pathway. See DOI: 10.1039/b000000x/

- 1 K. A. Jacobson and G. Z. Gao, *Nat. Rev. Drug Disc.*, 2006, **5**, 247–264.
- 2 S. Latini and F. Pedata, *J. Neurochem.*, 2001, **79**, 463–484.
- 3 A. M. Sebastiao, J. A. Ribeiro, *Trends Pharmacol. Sci.*, 2000, **21**, 341–346.
- 4 B. B. Fredholm, K. A. Jacobson, J. Linden, C. E. Muller, *Pharmacol. Rev.*, 2011, **63**, 1–34.
- 5 G. Lebon, T. Warne, P. C. Edwards, K. Bennett, C. J. Langmead, A. G. Leslie, C. G. Tate, *Nature*, 2011, **474**, 521–525.
- 6 D. Sabbadin, S. Moro, *J. Comp. Inf. Mod.*, 2014, **54**, 372–376.
- 7 S. Moro, C. Hoffmann, K. A. Jacobson, *Biochemistry*, 1999, **38**, 3498–3507.
- 8 H. Keränen, H. Gutiérrez-de-Terán, J. Åqvist, *PLOS ONE*, 2014, **9**, e108492.
- 9 J. A. Ballesteros and H. Weinstein, in *Methods Neurosci.*, ed. Stuart C. Sealfon, Academic Press, 1995, vol. Volume **25**, pp. 366–428.
- 10 W. Humphrey, A. Dalke and K. Schulten, *J. Mol. Graph.*, 1996, **14**, 33–38, 27–28.
- 11 M. Seeber, A. Felling, F. Raimondi, S. Muff, R. Friedman, F. Rao, A. Caflisch and F. Fanelli, *J Comput Chem*, 2011, **32**, 1183–1194.
- 12 A. D. MacKerell Jr, N. Banavali and N. Foloppe, *Biopolymers*, 2000, **56**, 257–265.
- 13 J. C. Phillips, R. Braun, W. Wang, J. Gumbart, E. Tajkhorshid, E. Villa, C. Chipot, R. D. Skeel, L. Kalé and K. Schulten, *Journal of Computational Chemistry*, 2005, **26**, 1781–1802.
- 14 Acellera, www.acellera.com
- 15 H. M. Berman, J. Westbrook, Z. Feng, G. Gilliland, T. N. Bhat, H. Weissig, I. N. Shindyalov and P. E. Bourne, *Nucl. Acids Res.*, 2000, **28**, 235–242.
- 16 The UniProt Consortium, *Nucleic Acids Res.*, 2010, **38**, D142–148.
- 17 E. Jain, A. Bairoch, S. Duvaud, I. Phan, N. Redaschi, B. E. Suzek, M. J. Martin, P. McGarvey and E. Gasteiger, *BMC Bioinformatics*, 2009, **10**, 136.
- 18 S. F. Altschul, T. L. Madden, A. A. Schäffer, J. Zhang, Z. Zhang, W. Miller and D. J. Lipman, *Nucleic Acids Res.*, 1997, **25**, 3389–3402.
- 19 Chemical Computing Group, www.chemcomp.com.
- 20 P. Labute, *Proteins*, 2009, **75**, 187–205.

Journal Name

- 21 M. A. Lomize, A. L. Lomize, I. D. Pogozeva and H. I. Mosberg, *Bioinformatics*, 2006, **22**, 623–625.
- 22 W. L. Jorgensen, J. Chandrasekhar, J. D. Madura, R. W. Impey and M. L. Klein, *J. Chem. Phys.*, 1983, **79**, 926–935.
- 23 Helmut Grubmüller and Volker Groll, *Solvate* 1.0.1. <http://www.mpibpc.mpg.de/grubmueller/solvate>, 1996-2010.
- 24 K. Vanommeslaeghe and A. D. MacKerell, *J. Chem. Inf. Model.*, 2012, **52**, 3144–3154.
- 25 K. Vanommeslaeghe, E. P. Raman and A. D. MacKerell, *J. Chem. Inf. Model.*, 2012, **52**, 3155–3168.
- 26 V. Kräutler, W. F. van Gunsteren and P. H. Hünenberger, *J. Comput. Chem.*, 2001, **22**, 501–508.
- 27 U. Essmann, L. Perera, M. L. Berkowitz, T. Darden, H. Lee and L. G. Pedersen, *The J. Chem. Phys.*, 1995, **103**, 8577–8593.
- 28 W. J. Allen, J. A. Lemkul and D. R. Bevan, *J. Comput. Chem.*, 2009, **30**, 1952–1958.
- 29 N. Kucerka, S. Tristram-Nagle and J. F. Nagle, *J. Membr. Biol.*, 2005, **208**, 193–202.